PHYSICAL REVIEW D **89,** 116005 (2014)

Charmonium meson and hybrid radiative transitions

Peng Guo,[1,2,*] Tochtli Yépez-Martínez,[2] and Adam P. Szczepaniak[1,2,3]

[1]*Thomas Jefferson National Accelerator Facility, Newport News, Virginia 23606, USA*
[2]*Center for Exploration of Energy and Matter, Indiana University, Bloomington, Indiana 47408, USA*
[3]*Physics Department, Indiana University, Bloomington, Indiana 47405, USA*

(Received 3 March 2014; published 5 June 2014)

We consider the nonrelativistic limit of the QCD Hamiltonian in the Coulomb gauge, to describe radiative transitions between conventional charmonium states and from the lowest multiplet of $c\bar{c}$ hybrids to charmonium mesons. The results are compared to potential-quark models and lattice calculations.

DOI: 10.1103/PhysRevD.89.116005 PACS numbers: 11.10.Ef, 12.38.Lg, 12.39.Hg, 12.40.-y

I. INTRODUCTION

It has long been stipulated that excitation of the gluon field would appear in the spectrum of hadrons. Hybrid resonances, i.e. states that contain both quark and gluon excitations, were considered in various models [1–6], and recent lattice simulations [7–9] have provided solid theoretical evidence for such states. Moreover, in recent years several new states, in particular in the charmonium spectrum, have been discovered possibly including a hybrid resonance, the $Y(4260)$. Conventional heavy quarkonia are well described by nonrelativistic QCD [10]. Thus it is reasonable to expect that hybrids containing heavy quarks could be treated in a similar way, i.e. by considering gluon excitations in the presence of slowly moving quarks. In physical gauges, e.g. the Coulomb gauge, dynamical gluons can be separated from the instantaneous Coulomb-type forces that act between color charges [11–17]. The non-Abelian Coulomb potential is expected to be responsible for binding and confinement [18,19] while the remaining, transverse gluon excitations could contribute to the spectrum.

To a good approximation heavy quarks interact with photons as bare Dirac particles. Thus radiative transitions can be used to explore quarkonium dynamics. We assume that this phenomenology can be extended to quarkonium hybrids. Over the years several radiative transitions involving charmonia have been measured [20–22] and extensive theoretical studies were performed [23–26]. More recently lattice gauge simulations have become available [27,28] and these also include predictions for transitions involving hybrid mesons [29,30].

In this work we focus on radiative transitions involving lowest mass conventional charmonia and the lowest mass multiplet of charmonium hybrids. The ordinary $c\bar{c}$ states we consider have quark orbital angular momentum and spin restricted to the lowest values, of L, $S = 0$, 1, that result in states with angular momentum, parity and charge conjugation, $J^{PC} = 0^{-+}$, 1^{--}, 1^{+-}, $(0,1,2)^{++}$. In the nonrelativistic, Coulomb gauge QCD the lowest mass charmonium hybrid multiplet is predicted to contain a color-octet $c\bar{c}$ pair with $J_q^{P_q C_q} = 0^{-+}$ or 1^{--} corresponding to the total quark-antiquark spin $S = 0$ and $S = 1$, respectively, coupled to a single quasigluon. This physical, transverse gluon is predicted to have quantum numbers, $J_g^{P_g C_g} = 1^{+-}$. The unusual, positive parity of the gluon originates from the non-Abelian nature of the Coulomb interactions [14,15]. Coupling of the $c\bar{c}$ and the gluon produces a multiplet containing four hybrid states, with overall quantum numbers of $J^{PC} = 1^{--}$, $(0,1,2)^{-+}$. This four state multiplet has been recently identified in lattice simulations, both in the heavy and light quark sectors. It includes the exotic state with $J^{PC} = 1^{-+}$ and three states with nonexotic quantum numbers, 1^{--}, 0^{-+}, 2^{-+}. The gluon content of the former was identified trough determination of matrix elements of operators containing gluon fields [27,29,30].

The paper is organized as follows. In Sec. II we detail the Coulomb gauge approach to conventional charmonium radiative transitions and to transitions involving hybrid mesons. We discuss the basis states for ordinary $c\bar{c}$ mesons and $c\bar{c}g$ hybrids and the corresponding transition matrix elements. In Sec. III a multipole analysis of the radiative transitions is presented. We also discuss current matrix elements involving states of identical charge conjugation. These vanish when a photon couples to both the quark and the antiquark but are in general finite when the current operator acts on a single quark. They are well defined within the model and have also been computed on the lattice. Summary and outlook are given in Sec. IV and all details of derivations are given in the appendixes.

II. QUARKONIUM STATES IN THE COULOMB GAUGE

The QCD Hamiltonian $H_{\rm QCD}$, which describes nonrelativistic quarks interacting with (relativistic) gluons, can be constructed from the full QCD Hamiltonian in the Coulomb gauge by applying Foldy-Wouthuysen transformation [31]. This Hamiltonian was used to study the

*pguo@jlab.org

gluelump spectrum [14] and the low mass charmonia and bottomonia including hybrids [15]. In addition to the strong interaction part, here we also consider the minimal coupling of the photon to the quarks, which in the nonrelativistic limit is given by

$$H_{\rm QED} = \frac{e_q}{2m}\int d\mathbf{x}\Psi^\dagger(\mathbf{x})\beta[2i\mathbf{A}_\gamma(\mathbf{x})\cdot\nabla - \Sigma\cdot\mathbf{B}_\gamma(\mathbf{x})]\Psi(\mathbf{x}), \tag{1}$$

where $\mathbf{A}_\gamma$ and $\mathbf{B}_\gamma$ are the photon vector potential and magnetic field, respectively. The quark fields are related to particle operators by

$$\Psi^i(\mathbf{x}) = \sum_{\lambda=\pm1/2}\int\frac{d\mathbf{k}}{(2\pi)^3}e^{i\mathbf{k}\cdot\mathbf{x}}[u_\lambda b(\mathbf{k},\lambda,i) + v_\lambda d^\dagger(-\mathbf{k},\lambda,i)] \tag{2}$$

with u, v being the Dirac spinors in the nonrelativistic limit. Given an (approximate) solution of the Schrödinger equation

$$H_{\rm QCD}|N[c\bar{c}]\rangle = E_N|N[c\bar{c}]\rangle \tag{3}$$

within the Fock sector containing only the heavy quark-antiquark pair the QED interaction of Eq. (1) determines the radiative transition matrix element,

$$\mathcal{M}_{N\to N'\gamma} \propto \langle N'[c\bar{c}],\gamma|H_{\rm QED}|N[c\bar{c}]\rangle \tag{4}$$

between ordinary charmonia. In the case of transitions involving hybrids, which are given by solutions of

$$H_{\rm QCD}|N[c\bar{c}g]\rangle = E_N|N[c\bar{c}g]\rangle \tag{5}$$

in the sector containing in addition to the $c\bar{c}$ pair a transverse quasigluon, the radiative transition to an ordinary meson state has to be accompanied by gluon absorption. To lowest order in the heavy quark mass expansion the latter is determined by the instantaneous Coulomb interaction that changes the gluon number, $\langle c\bar{c}|H_C|c\bar{c}g\rangle$. Here H_C is given by

$$H_C = -\frac{g^2}{2}\int d\mathbf{x}d\mathbf{y}\rho^a(\mathbf{x})K_{a,b}(\mathbf{x},\mathbf{y},\mathbf{A}_g)\rho^b(\mathbf{y}), \tag{6}$$

$\rho^a(\mathbf{x}) = \Psi^\dagger(\mathbf{x})T^a\Psi(\mathbf{x})$ is the quark color charge density and the gluon field $\mathbf{A}_g$ is related to the quasigluon particle operators by

$$\mathbf{A}_g^a(\mathbf{x}) = \int\frac{d\mathbf{k}}{(2\pi)^3}\frac{e^{i\mathbf{k}\cdot\mathbf{x}}}{\sqrt{2\omega(k)}}[\boldsymbol{\epsilon}(\mathbf{k},\lambda)a(\mathbf{k},\lambda,a) + \boldsymbol{\epsilon}^\dagger(-\mathbf{k},\lambda)a^\dagger(-\mathbf{k},\lambda,a)], \tag{7}$$

with λ, a being the helicity and color indices, respectively, and $\boldsymbol{\epsilon}(\mathbf{k},\lambda)$ the helicity vectors. The quasigluon orbitals and the quasigluons' dispersion function $\omega_k = \omega(k)$ have been studied elsewhere using a variational model for the QCD vacuum [15]. In the variational model the Coulomb kernel is replaced by its vacuum expectation value and the operator which changes the gluon number by one becomes

$$K_{a,b} = f^{abc}\int\frac{d\mathbf{k}}{(2\pi)^3}\frac{d\mathbf{q}}{(2\pi)^3}e^{i\mathbf{k}\mathbf{x}-i\mathbf{q}\cdot\mathbf{y}}\mathbf{k}\cdot\mathbf{A}_g^c(\mathbf{k}-\mathbf{q})K^1(k,q) \tag{8}$$

with the scalar function $K^1(k,q)$ obtained from a solution of a series of Dyson-Schwinger equations [32–38]. The model has been used successfully [39,40] in the study of excited adiabatic potentials between static quarks [41], which can be used to determine the single gluon orbitals in Eq. (7). Combining Eqs. (1) and (6) leads to effective operators for radiative transitions between hybrid and ordinary quarkonia

$$\mathcal{M}_{N\to N'\gamma} \propto \langle N'[c\bar{c}],\gamma|H^{\rm eff}_{\rm QED}|N[c\bar{c}g]\rangle, \tag{9}$$

where

$$H^{\rm eff}_{\rm QED} = \frac{1}{2}\frac{H_C H_{\rm QED}}{\Delta E} \tag{10}$$

with $1/\Delta E$ representing the Green's function of the $c\bar{c}$ pair. In the following we calculate the matrix elements $\mathcal{M}$ and the decay widths for several hybrid states. As discussed previously, we focus on the hybrid states containing quark and antiquark angular momentum $L = 0,\ 1$ and spin $S = 0,\ 1$. In particular we investigate transitions involving the hybrid with exotic quantum numbers $\eta_{c1}(1^{-+})$. This state has been described by lattice calculations [27,29] and is expected to have a mass around 4.3 GeV.

A. Meson basis and matrix elements

We represent the Nth quarkonium state of spin J and its projection M, with parity P, charge conjugation C and total momentum $\mathbf{P}$, as

$$|\mathbf{P};JMPCN\rangle = \sum_{\alpha,m_1,m_2}\int\frac{d\mathbf{q}}{(2\pi)^3}\Psi^{N,\alpha}_{c\bar{c}}(q) \times\chi^{JMPC}_{m_1,m_2}(\hat{\mathbf{P}},\hat{\mathbf{q}},\alpha)b^\dagger(\mathbf{p}_c,m_1,i_1)\frac{\delta_{i_1,i_2}}{\sqrt{N_c}}d^\dagger(\mathbf{p}_{\bar{c}},m_2,i_2)|0\rangle. \tag{11}$$

Here $\alpha = (L,S)$, and q is the magnitude of relative momentum between quark and antiquark. $\mathbf{p}_c = \frac{\mathbf{P}}{2}+\mathbf{q}$ and $\mathbf{p}_{\bar{c}} = \frac{\mathbf{P}}{2}-\mathbf{q}$ are the quark and antiquark momenta respectively. The meson spin-orbital wave function is written using the L-S coupling scheme with L, and S

the orbital angular momentum and spin of the quark-antiquark, respectively,

$$\chi^{JMPC}_{m_1,m_2}(\hat{\mathbf{P}},\hat{\mathbf{q}},\alpha) = \sum_{M_S,M_L} Y_{LM_L}(\hat{\mathbf{q}})\left\langle \frac{1}{2}m_1;\frac{1}{2}m_2|SM_S\right\rangle \times \langle SM_S;LM_L|JM\rangle \frac{1+C(-1)^{L+S}}{2}\frac{1+P(-1)^{L+1}}{2}. \quad (12)$$

The states are normalized according to

$$\langle \mathbf{P}';J'M'P'C'N'|\mathbf{P};JMPCN\rangle = 2E_{c\bar{c}}(2\pi)^3\delta^3(\mathbf{P}-\mathbf{P}')\delta_{JJ'}\delta_{MM'}\delta_{PP'}\delta_{CC'}\delta_{NN'}. \quad (13)$$

As mentioned before the meson-to-meson radiative transitions are calculated with the minimal coupling of the photon to the quarks; cf. Eq. (1). Explicitly, the matrix elements are given by

$$\mathcal{M}_{N\to N'\gamma} = -\frac{e_q}{2m_q(2\pi)^3}\int d\mathbf{q}d\mathbf{q}'\Psi^{N,\alpha}_{c\bar{c}}(q)\Psi^{N',\alpha'}_{c\bar{c}}(q')\sum_{m_1,m_2,m_1',m_2'}\chi^{*JMPC}_{m_1,m_2}(\hat{\mathbf{q}},\alpha)\chi^{J'M'P'C'}_{m_1',m_2'}(\hat{\mathbf{q}}',\alpha')\epsilon(\mathbf{k}_\gamma,\sigma_\gamma) \cdot\left[\delta\left(\mathbf{q}'-\mathbf{q}+\frac{\mathbf{k}_\gamma}{2}\right)(2\mathbf{q}'+i\sigma\times\mathbf{k}_\gamma)_{m_1,m_1'}\delta_{m_2m_2'}+\delta\left(\mathbf{q}-\mathbf{q}'+\frac{\mathbf{k}_\gamma}{2}\right)(2\mathbf{q}'+i(\sigma_2\sigma\sigma_2)\times\mathbf{k}_\gamma)_{m_2',m_2}\delta_{m_1m_1'}\right]. \quad (14)$$

The spin-orbital wave function $\chi^{JMPC}_{m_1,m_2}(\hat{\mathbf{q}},\alpha)$ for charmonium mesons $J^{PC}=0^{-+}$, 1^{--}, 1^{+-}, $(0,1,2)^{++}$ are tabulated in Appendix A.

B. Hybrid basis and transition matrix elements

It is reasonable to assume that wave function of hybrids with nonrelativistic quarks are similar to those of gluelumps which contain static quarks. In the construction of hybrid wave functions we thus follow the coupling scheme optimized for gluelump studies [14]. The $Q\bar{Q}g$ state is obtained by initially coupling the $Q\bar{Q}$ relative angular momentum L to the total gluon spin J_g. The resulting angular momentum j is then coupled to the total quark-antiquark spin S to give the total spin of the hybrid state J. The hybrid state with total spin J, spin projection M, parity P, charge conjugation C is then given by

$$|JMPCN\rangle = \sum_{\alpha=(J_gS,L,j)}\int\frac{d\mathbf{k}}{(2\pi)^3}\frac{d\mathbf{q}}{(2\pi)^3}\Psi^{N,\alpha}_{c\bar{c}g}(k,q)\sum_{m_1,m_2,\sigma}\frac{1}{\sqrt{C_FN_c}}\chi^{JMPC}_{m_1,m_2,\sigma}(\hat{\mathbf{k}},\hat{\mathbf{q}},\alpha) \times b^\dagger\left(\frac{\mathbf{k}}{2}+\mathbf{q},m_1,i_1\right)T^a_{i_1,i_2}d^\dagger\left(\frac{\mathbf{k}}{2}-\mathbf{q},m_2,i_2\right)a^\dagger(-\mathbf{k},\sigma,a)|0\rangle. \quad (15)$$

Here $\mathbf{q}$ is the relative momentum between the quark-antiquark and $\mathbf{k}$ is the momentum of the gluon in the overall center of mass frame. The spin-orbital wave function $\chi^{JMPC}_{m_1,m_2,\sigma}(\hat{\mathbf{k}},\hat{\mathbf{q}},\alpha)$ describes the $(\boldsymbol{L}+\boldsymbol{J}_g)+\boldsymbol{S}$ coupling and $\sigma=\pm1$ represents the gluon helicity

$$\chi^{JMPC}_{m_1,m_2,\sigma}(\hat{\mathbf{k}},\hat{\mathbf{q}},\alpha) = \sqrt{\frac{2J_g+1}{4\pi}}\frac{1+C(-1)^{L+S+1}}{2}\sum_{M_S,M_L,M_g,m}Y_{LM_L}(\mathbf{q})\left\langle\frac{1}{2}m_1,\frac{1}{2}m_2|SM_S\right\rangle \times\langle J_gM_g,LM_L|jm\rangle\langle jm,SM_S|JM\rangle\frac{(-1)^{J_g}}{\sqrt{2}}D^{*J_g}_{M_g,-\sigma}(\hat{\mathbf{k}})[\delta_{\sigma,1}+P(-1)^{J_g+L+1}\delta_{\sigma,-1}]. \quad (16)$$

The parity and charge conjugation are given by

$$P=\xi(-1)^{J_g+L+1}, \qquad C=(-1)^{L+S+1}, \quad (17)$$

respectively. Here $\xi=+1$ corresponds to the transverse magnetic (TM) (natural parity) and $\xi=-1$ for the transverse electric (TE) (unnatural parity) gluon states that are given to be $|\sigma=+1\rangle+\xi|\sigma=-1\rangle$ combinations of gluon helicity states. As expected, both P and C are a product of the $Q\bar{Q}$ and gluon parity and charge conjugation are given by

$$P_q=(-1)^{L+1}, \qquad P_g=\xi(-1)^{J_g}$$
$$C_q=(-1)^{L+S}, \qquad C_g=-1. \quad (18)$$

The state is normalized in the same way as the normalization of the conventional meson state in Eq. (13). For the

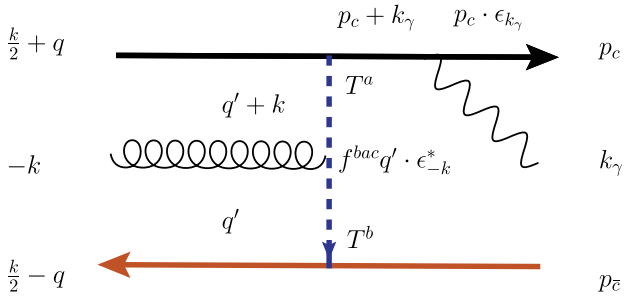

FIG. 1 (color online). Diagrammatic representation of one possible configuration for hybrid-to-meson radiative transitions contributing to the matrix element in Eq. (19).

lowest four hybrids we are considering [15], $(L, J_g^{P_g C_g}) = (0, 1^{+-})$, which correspond to the gluon in the TE mode. Coupling the TE gluon with the color octet $Q\bar{Q}$ state in $L = 0$ produces a hybrid state with the intermediate angular momentum $\mathbf{j} = \mathbf{L} + \mathbf{J}_g = 1$. Adding the quark spin $S = 0, 1$, and ignoring hyperfine splitting we obtain four low lying hybrids with quantum numbers, $J^{PC} = 1^{--}$ for $S = 0$ and $J^{PC} = 0^{-+}, 1^{-+}, 2^{-+}$ for $S = 1$. It is worth noting that the hybrid with exotic quantum numbers 1^{-+} appears in this lowest multiplet and is predicted to have the $Q\bar{Q}$ pair in spin 1.

The matrix elements for the hybrid-to-meson radiative transition are given by

$$\mathcal{M}_{N\to N'\gamma} = \frac{e_q g^2}{4m_q}\frac{N_c\sqrt{C_F}}{\sqrt{2}}\int \frac{d\mathbf{k}}{(2\pi)^3}\frac{d\mathbf{q}}{(2\pi)^3}\frac{d\mathbf{q}'}{(2\pi)^3}\Psi^{N,\alpha}_{c\bar{c}g}(k,q)\Psi^{N',\alpha'}_{c\bar{c}}(q')\frac{1}{\sqrt{\omega_{k_\gamma}\omega_k}\Delta E}$$
$$\times \sum_{m_1 m_2\sigma}\sum_{m_1' m_2'}\chi^{*JMPC}_{m_1,m_2,\sigma}(\hat{\mathbf{k}},\hat{\mathbf{q}},\alpha)\chi^{J'M'P'C'}_{m_1',m_2'}(\hat{\mathbf{q}}',\alpha')\int d\mathbf{q}_g \mathbf{q}_g\cdot\epsilon^*(-\mathbf{k},\sigma)K^{(1)}\left(\left|\frac{\mathbf{k}}{2}+\mathbf{q}_g\right|,\left|\frac{\mathbf{k}}{2}-\mathbf{q}_g\right|\right)$$
$$\times \epsilon(\mathbf{k}_\gamma,\sigma_\gamma)\cdot\left\{\delta\left(\mathbf{q}+\mathbf{q}_g-\mathbf{q}'-\frac{\mathbf{k}_\gamma}{2}\right)\left[2\left(\mathbf{q}'+\frac{\mathbf{k}}{4}-\frac{\mathbf{q}_g}{2}\right)+i\sigma\times\mathbf{k}_\gamma\right]_{m_1,m_1'}\delta_{m_2 m_2'}\right.$$
$$\left.+\,\delta\left(\mathbf{q}+\mathbf{q}_g-\mathbf{q}'+\frac{\mathbf{k}_\gamma}{2}\right)\left[2\left(\mathbf{q}'-\frac{\mathbf{k}}{4}-\frac{\mathbf{q}_g}{2}\right)+i(\sigma_2\sigma\sigma_2)\times\mathbf{k}_\gamma\right]_{m_2',m_2}\delta_{m_1 m_1'}\right\}. \quad (19)$$

The explicit forms of the spin-wave functions are summarized in Appendix A. In Fig. 1, we illustrate one of the four possible ways of coupling the photon to a quark line.

III. RADIATIVE TRANSITIONS: NUMERICAL RESULTS AND DISCUSSION

A. Conventional mesons

We have considered a total of fifteen transitions between conventional charmonia. Even though some of the transitions considered here vanish due to charge conjugation, we investigate the underlying matrix elements with a photon attached to only one of the quarks. Some of these C-violating results can be compared with lattice results reported in [29], and others constitute our predictions. Using the model described in Sec. II, we present below the final expressions for the matrix elements and decay widths computed from

$$\Gamma(N\to N'\gamma) = \int d\Omega_\gamma \frac{1}{32\pi^2}\frac{k_\gamma}{m_N^2}\frac{1}{2J_N+1}$$
$$\times \sum_{\sigma_\gamma, M_N, M_{N'}}|\mathcal{M}_{N\to N'\gamma}|^2. \quad (20)$$

A summary of numerical results is given in Table I, including ratios of decay widths relative to $\Gamma(\chi_{c_2}\to\gamma J/\psi)$, e.g. $R_{N\to N'} \equiv \Gamma(N\to N'\gamma)/\Gamma(\chi_{c_2}\to\gamma J/\psi)$, which are compared to model calculations from [26]. We also discuss the transition amplitudes $|\hat{V}|$ and $|\hat{F}_k|$ introduced in [27,29] in the context of analysis of lattice data. Here $\hat{F}_k$ represents either an electric, $\hat{E}_k$, or magnetic, $\hat{M}_k$, multipole and $\hat{V}$ is the dipole magnetic multipole for the transition involving a vector and a pseudoscalar meson,

$$|\hat{F}|^2 = |\hat{F}_1|^2 = \frac{1}{8e_q^2}\sum_{\sigma_\gamma, M_N, M_{N'}}|\mathcal{M}_{N\to N'\gamma}|^2,$$
$$|\hat{V}|^2 = \frac{(m_N+m_{N'})^2}{32e_q^2 m_N^2 k_\gamma^2}\sum_{\sigma_\gamma, M_N, M_{N'}}|\mathcal{M}_{N\to N'\gamma}|^2. \quad (21)$$

For the radial wave functions we use a harmonic oscillator approximation with a width parameter $\beta = 0.5$ GeV. This leads to some differences with respect to the other potential-quark results of [26], where Coulomb plus linear plus hyperfine interactions were used to compute the wave functions. Sensitivity of the radiative transitions to the short-range correlations have motivated precision calculations, which can, for example, be carried out in perturbation theory and are summarized in the recent reviews [42,43]. Finally, we calculate the transition amplitudes for charge conjugation–violating transitions, $|\hat{F}|/2$. The factor of 2 is introduced to account for the fact that a photon couples to a single quark. Our findings are summarized below.

TABLE I. Conventional $c\bar{c}$ meson transitions compared to NR-potential model, lattice calculations and the PDG values, when available. The charge-violating transitions described in the text are denoted by CV. The input charmonium meson masses have been taken from the nonrelativistic model of [26]. The width parameter in the present model is fixed at $\beta = 0.5$ GeV and the ratio R is defined in the text.

Transition	k_γ (MeV)	R	R [26]	TA (GeV)	(TA, β) (GeV) [27,29]	Γ (keV)	Γ (keV) [44]
$(\chi_{c_2} \to h_c\gamma)_{M_1}$	40	3.2×10^{-4}	⋯	$\lvert\hat{F}\rvert = 0.12$	⋯	0.1	⋯
$(\chi_{c_2} \to \chi_{c1}\gamma)_{CV}$	45	0	⋯	$\lvert\hat{F}\rvert_{CV} = 0.10$	⋯	0	⋯
$(\chi_{c_2} \to \chi_{c0}\gamma)_{CV}$	138	0	⋯	0	⋯	0	⋯
$(\chi_{c_2} \to J/\psi\gamma)_{E_1}$	429	1	1	$\lvert\hat{F}\rvert = 2.02$	$(\lvert\hat{F}\rvert = 1.97, 0.55)$	363	380
$(\chi_{c_2} \to \eta_c\gamma)_{CV}$	530	0	⋯	0	⋯	0	⋯
$(h_c \to \chi_{c_1}\gamma)_{M_1}$	5	$\sim 10^{-7}$	⋯	$\lvert\hat{F}\rvert = 0.01$	⋯	$\sim 10^{-3}$	⋯
$(h_c \to \chi_{c_0}\gamma)_{M_1}$	100	1.7×10^{-3}	⋯	$\lvert\hat{F}\rvert = 0.13$	⋯	0.6	⋯
$(h_c \to J/\psi\gamma)_{CV}$	394	0	⋯	0	⋯	0	⋯
$(h_c \to \eta_c\gamma)_{E_1}$	504	1.14	1.17	$\lvert\hat{E}_1\rvert = 1.54$	$(\lvert\hat{E}_1\rvert = 1.85, 0.69)$	416	372
$(\chi_{c_1} \to \chi_{c0}\gamma)_{CV}$	95	0	⋯	$\lvert\hat{F}\rvert_{CV} = 0.17$	⋯	0	⋯
$(\chi_{c_1} \to J/\psi\gamma)_{E_1}$	390	0.92	0.74	$\lvert\hat{E}_1\rvert = 1.56$	$(\lvert\hat{E}_1\rvert = 1.88, 0.56)$	333	302
$(\chi_{c_1} \to \eta_c\gamma)_{CV}$	492	0	⋯	0	⋯	0	⋯
$(\chi_{c_0} \to J/\psi\gamma)_{E_1}$	303	0.73	0.36	$\lvert\hat{E}_1\rvert = 1.33$	$(\lvert\hat{E}_1\rvert = 0.83, 0.54)$	265	123
$(\chi_{c_0} \to \eta_c\gamma)_{CV}$	408	0	⋯	0	⋯	0	⋯
$(J/\psi \to \eta_c\gamma)_{M_1}$	116	7.9×10^{-3}	6.8×10^{-3}	$\lvert\hat{V}\rvert = 1.98/\text{GeV}$	$(\lvert\hat{V}\rvert = 1.85/\text{GeV}, 0.54)$	2.9	1.5

1. $\chi_{c2}(2^{++}) \to h_c(1^{+-})\gamma$

A summary of recent experimental results on the decays of charmonium can be found in [45]. To the best of our knowledge, however, this transition has not been measured. It corresponds to a magnetic dipole, which in general is expected to be weaker than the electric dipole transition. The matrix element corresponding to the dominant, M_1 transition is given by

$$\mathcal{M}_{N\to N'\gamma} = -\frac{e_q}{m_q}\frac{3i}{4\pi}\epsilon_M^{*ij}[\mathbf{k}_\gamma \times \epsilon(\mathbf{k}_\gamma, \sigma_\gamma)]^i \epsilon^j_{M'}\mathcal{A}, \qquad (22)$$

where m_q and $e_q = (2/3)\sqrt{4\pi\alpha_{em}}$ are the charm quark mass and charge, respectively. Here ϵ^{ij}_M and ϵ^i_M are the spin-2 and spin-1 polarization vectors, respectively, and the scalar function $\mathcal{A}$ is given in Appendix B. Using the harmonic oscillator wave function we obtain $\Gamma = 0.1$ keV. The difference with respect to the expressions given in [26] can be traced to an intrinsic ambiguity in normalization of the wave functions, i.e. the difference is of the order of $E_f^{c\bar{c}}/M_i^{c\bar{c}} - 1$. A more extended theoretical and experimental report on heavy quarkonium physics is given in [46], where the effects of higher order relativistic corrections are discussed.

2. $\chi_{c2}(2^{++}) \to J/\psi(1^{--})\gamma$

This tensor-to-vector transition has been studied in potential-quark models [25,26] and also on the lattice [29]. There is experimental evidence for transitions involving radial excitations of the tensor states $\chi'_{c2} \to J/\psi\gamma$ and $\chi''_{c2} \to J/\psi\gamma$, but in this paper we focus on the ground state tensor, χ_{c2}. The corresponding matrix element is given by

$$\mathcal{M}_{N\to N'\gamma} = -\frac{e_q}{m_q}\frac{\sqrt{3}}{2\pi}\epsilon_M^{*ij}\epsilon^i_{M'}\epsilon^j(\mathbf{k}_\gamma\sigma_\gamma)\mathcal{D}, \qquad (23)$$

with $\mathcal{D}$ given in Appendix A. The multipole decomposition, Eq. (D1), yields an electric dipole E_1, magnetic quadrupole M_2 and electric octopole E_3, with E_1 being the leading one. The calculated value for the decay width of $\Gamma = 363$ keV in our model agrees with experimental data [44] and lattice calculations [29]. The FermiLab-E760 [47], BES Collaboration [48] and CLEO Collaboration [49] have all reported this transition. The PDG [44] reports a decay width $\Gamma = 380$ keV. The potential-quark models give a width within the range of $\Gamma \approx 289$–424 keV. The electric dipole transition amplitude value from lattice calculations is $\lvert\hat{F}\rvert = \lvert\hat{E}_1\rvert = 1.97$ GeV and it is obtained by extrapolating the electric dipole form factor to the physical photon point $\hat{E}_1(Q \to 0) = \hat{E}_1$. All results are summarized in Table I.

3. $h_c(1^{+-}) \to \chi_{c1}(1^{++})\gamma$

To the best of our knowledge there is no experimental information about this transition. The only observed transition between the $h_c(1^{+-})$ and another $c\bar{c}$ meson is $h_c(1^{+-}) \to \eta_c(0^{-+})\gamma$ [44], which we discuss later. The matrix element for this transition is given by

$$\mathcal{M}_{N\to N'\gamma} = \frac{e_q}{m_q}\frac{3}{4\pi\sqrt{2}}\varepsilon_{ijk}\varepsilon_{ilm}\epsilon_M^{*j}\epsilon^k_{M'}\mathbf{k}^l_\gamma\epsilon^m(\mathbf{k}_\gamma, \sigma_\gamma)\mathcal{A}. \qquad (24)$$

To leading order in photon momentum the M_1 transition dominates. We find $\Gamma = 239 \times 10^{-6}$ keV, which is small due to a limited phase space available for the decay.

4. $h_c(1^{+-}) \to \chi_{c0}(0^{++})\gamma$

Unlike the other transitions considered so far, the magnitude of photon momentum in this mode is large i.e. of the same order of magnitude as in the other measured magnetic dipole transition $J/\psi(1^{--}) \to \eta_c(0^{-+})\gamma$. The matrix element is given by

$$\mathcal{M}_{N\to N'\gamma} = \frac{e_q}{m_q}\frac{\sqrt{3}i}{4\pi}\epsilon_M^* \cdot [\mathbf{k}_\gamma \times \epsilon(\mathbf{k}_\gamma, \sigma_\gamma)]\mathcal{A}. \tag{25}$$

The multipole decomposition Eq. (D1) implies dominance of a magnetic dipole M_1. Because of the large photon momentum, $|k_\gamma| = 100$ MeV, for this decay we find $\Gamma = 0.6$ keV, which is comparable with the decay width expected for the magnetic dipole transition $\Gamma(J/\psi \to \eta_c\gamma)$.

5. $h_c(1^{+-}) \to \eta_c(0^{-+})\gamma$

This transition corresponds to the only observed transition involving the $h_c(1^{+-})$ meson. It has been observed by the CLEO Collaboration [50,51] and confirmed by the BESIII Collaboration [52].

The multipole decomposition Eq. (D1) implies an electric dipole E_1 transition. The matrix element can be expressed as

$$\mathcal{M}_{N\to N'\gamma} = -\frac{e_q}{m_q}\frac{2\sqrt{3}}{4\pi}\epsilon_M^* \cdot \epsilon(\mathbf{k}_\gamma, \sigma_\gamma)\mathcal{D}. \tag{26}$$

The experiment reports [44] $\Gamma = 372$ keV. The potential-quark models [25,26] report a decay width in the range $\Gamma \approx 352$–498 keV and lattice [27] reports $\Gamma \approx 601$–663 keV. Our model yields $\Gamma = 416$ keV, which is consistent with these results.

6. $\chi_{c1}(1^{++}) \to J/\psi(1^{--})\gamma$

This transition has been reported experimentally and it was studied on the lattice [27] with the latter giving a central value somewhat above the experimental data albeit with a sizable error. The results of our model seem to be in good agreement with experiment. The matrix element for this transition is given by

$$\mathcal{M}_{N\to N'\gamma} = \frac{e_q}{m_q}\frac{\sqrt{6}i}{4\pi}\epsilon_M^* \cdot [\epsilon_{M'} \times \epsilon(\mathbf{k}_\gamma, \sigma_\gamma)]\mathcal{D}. \tag{27}$$

The multipole decomposition Eq. (D1) implies that the electric dipole E_1 and the magnetic quadrupole M_2 are the two leading matrix elements. The experiment reports [44] $\Gamma = 302$ keV. The potential-quark models give the width within the range $\Gamma \approx 215$–314 keV. This model yields $\Gamma = 333$ keV.

7. $\chi_{c0}(0^{++}) \to J/\psi(1^{--})\gamma$

The multipole decomposition Eq. (D1) for this transition implies the leading transition is the dipole electric E_1. The matrix element for this transition is given by

$$\mathcal{M}_{N\to N'\gamma} = \frac{e_q}{m_q}\frac{1}{2\pi}\epsilon(\mathbf{k}_\gamma, \sigma_\gamma) \cdot \epsilon_{M'}\mathcal{D}. \tag{28}$$

The experiment reports [44] $\Gamma = 123$ keV. The potential-quark models report the decay width within the range $\Gamma \approx 105$–152 keV. We find the value $\Gamma = 265$ keV.

Our results indicate approximately the same decay width 265–363 GeV for all transitions that involve the charmonium multiplet $(0, 1, 2)^{++}$ decaying to the $J/\psi(1^{--})$. Experimental data [44], however, indicate that the decay width $\Gamma(\chi_{c0}(0^{++}) \to J/\psi\gamma)$ is approximately one third of $\Gamma(\chi_{c2}(2^{++}) \to J/\psi\gamma)$. The discrepancy is related to our simple approximation for the wave function, which ignores hyperfine and spin-orbit interactions [25,26]. This example demonstrates that charmonium transitions can indeed be used to pin down the quark wave function.

8. $J/\psi(1^{--}) \to \eta_c(0^{-+})\gamma$

This is a magnetic dipole vector-pseudoscalar transition between two 1 S states. The photon momentum for this transition is about 116 MeV and the transition amplitude $\hat{V}$ is calculated as is shown in Eq. (21).

The matrix element for this transition is given by

$$\mathcal{M}_{N\to N'\gamma} = -\frac{e_q}{m_q}\frac{i}{4\pi}\epsilon_M^* \cdot [\mathbf{k}_\gamma \times \epsilon(\mathbf{k}_\gamma, \sigma_\gamma)]\mathcal{J}, \tag{29}$$

where $\mathcal{J}$ is defined in Appendix B.

The experiment [44] reports $\Gamma(J/\psi \to \eta_c\gamma) = 1.5$ keV for this transition. The potential-quark model result is in the range $\Gamma \approx 1.9$–2.9 keV and we find $\Gamma = 2.9$ keV.

There are a few magnetic dipole transitions experimentally reported for charmonium below the $D\bar{D}$ threshold (3.73 GeV) [44]. These are given by $J/\psi(1S) \to \eta_c(1S)\gamma$, $\psi(2S) \to \eta_c(2S)\gamma$ and $\psi(2S) \to \eta_c(1S)\gamma$. The last two correspond to radial excitations of S states. In this work, we only consider ground states for charmonium.

C-violating meson-to-meson transitions.—In addition to the allowed transitions, we investigated possible charge conjugation violation matrix elements which include $\chi_{c1} \to \eta_c\gamma$, $\chi_{c1} \to \chi_{c0}\gamma$, $h_c \to J/\psi\gamma$, $\chi_{c2} \to \eta_c\gamma$, $\chi_{c2} \to \chi_{c0}\gamma$ and $\chi_{c2} \to \chi_{c1}\gamma$. The finite matrix element for these transitions is obtained when a photon is coupled to a single quark line. The dominant $O(k_\gamma)$ matrix elements are found for $\chi_{c1} \to \chi_{c0}\gamma$ and $\chi_{c2} \to \chi_{c1}\gamma$.

9. $\chi_{c1}(1^{++}) \to \chi_{c0}(0^{++})\gamma$

The one-quark-line matrix element for this transition is given by

$$\mathcal{M}_{N\to N'\gamma} = -\frac{e_q}{m_q}\frac{\sqrt{3}i}{4\pi\sqrt{2}}\epsilon_M^* \cdot [\mathbf{k}_\gamma \times \epsilon(\mathbf{k}_\gamma, \sigma_\gamma)]\mathcal{A}, \quad (30)$$

which according to Eq. (D1) corresponds to a magnetic dipole M_1. The value obtained in this model is $|\hat{F}|_{CV} = 0.17$ GeV, which corresponds to the magnetic dipole transition amplitude defined by

$$|\hat{F}|^2_{CV} = \frac{1}{2e_q^2}\sum_{\sigma_\gamma, M_N, M_{N'}} |\mathcal{M}_{N\to N'\gamma}|^2. \quad (31)$$

10. $\chi_{c2}(2^{++}) \to \chi_{c1}(1^{++})\gamma$

The one-quark-line matrix element for this transition is given by

$$\mathcal{M}_{N\to N'\gamma} = \frac{e_q}{m_q}\frac{3i}{8\pi\sqrt{2}}\varepsilon_{ikl}\varepsilon_{jml}\epsilon_M^{*ij}\epsilon_{M'}^m[\mathbf{k}_\gamma \times \epsilon(\mathbf{k}_\gamma, \sigma_\gamma)]^k\mathcal{A}, \quad (32)$$

which according to Eq. (D1) corresponds to M_1, E_2 and M_3 transitions. For $|\hat{F}|_{CV}$ defined in Eq. (31) we obtain $|\hat{F}|_{CV} = 0.10$ GeV.

In Table I we summarize our findings and compare with the nonrelativistic potential-quark model of [26] and, when available, with the transition amplitudes $TA = |\hat{F}|$, $|\hat{V}|$ from lattice computations [27,29]. We use a single scale parameter for all wave functions, while in the analysis of lattice data the scale is fitted independently for each transition. The specific values are shown in Table I. The photon momentum for each transition is given by $k_\gamma = (M_N^2 - M_{N'}^2)/2M_N$.

B. Hybrid-to-meson radiative decays

We have studied 24 possible hybrid-to-meson radiative transitions, including matrix elements for C-violating modes. The results are discussed below. In Table II, we quote the expected decay ratios for these transitions when using $m_{hyb} = 4.35$ GeV for the spin-averaged mass of the lowest hybrid multiplet $1^{--}, (0,1,2)^{-+}$. To minimize sensitivity to the wave functions we also quote the ratio of hybrid decay amplitudes computed in the model, cf. Eq. (21), to those computed using lattice simulations [29]. Specifically, from lattice simulations two widths are quoted. The $Y(1^{--}) \to \eta_c\gamma$ transition from a hybrid vector, Y, is a magnetic dipole with the decay width given by

$$\Gamma(Y \to \eta_c\gamma) = \alpha k_\gamma^3 \frac{64}{27}\frac{|\hat{V}|^2}{(m_Y + m_{\eta_c})^2}, \quad (33)$$

where the magnetic dipole matrix element $\hat{V} = 0.28$ yields $\Gamma(Y \to \eta_c\gamma) = 42$ keV. The second transition reported in [29] is $\eta_{c_1}(1^{-+}) \to J/\psi(1^{--})\gamma$ from the exotic hybrid η_{c_1}, which is also of a magnetic dipole type, with the decay width given by

$$\Gamma(\eta_{c_1} \to J/\psi\gamma) = \alpha k_\gamma \frac{16}{27}\frac{|\hat{F}|^2}{m^2_{\eta_{c1}}}, \quad (34)$$

and the matrix element, $\hat{F} = 0.69$ GeV, gives $\Gamma(\eta_{c1} \to J/\psi\gamma) = 115$ keV. As it is shown below, all hybrid transition amplitudes in our model depend on a single factor $|\mathcal{Z}_0|$ that is determined by the hybrid meson wave function. We will use the two magnetic dipole matrix elements, $\hat{M}_1$ and $\hat{F}$, to normalize this factor to make predictions for transitions not yet reported but calculable in our model.

For the C-violating matrix elements we will use the transition $1^{-+} \to 0^{++}\gamma$ from [29] to normalize the relevant wave function overlap factor in our model.

1. $Y(1^{--}) \to \eta_c(0^{-+})\gamma$

This transition involves a hybrid vector meson state denoted as Y. Lattice simulations of charmonium (as well as light quark mesons) predict a vector state located between first and second resonance region i.e. above the first radial and orbital excitation of the ground state spin-1 $q\bar{q}$. Experimentally the $Y(4260)$ is a possible candidate for this hybrid in the charmonium spectrum and the $Y(2175)$ is the hybrid candidate in the $s\bar{s}$ sector [53]. The transition between a hybrid vector and ordinary pseudoscalar $c\bar{c}$ meson is of magnetic dipole type. In magnetic transitions between conventional, vector charmonium and the η_c there is no change in angular momentum, but instead, the transition involves a quark spin flip. In contrast, because of presence of gluon spin, the magnetic transition from a hybrid vector does not require a quark spin flip. This picture is supported by the lattice results [29].

The matrix elements are given by

$$\mathcal{M}_{N\to N'\gamma} = \frac{e_q}{m_q}\frac{3i}{64\pi^{\frac{3}{2}}}\epsilon_M^* \cdot [\mathbf{k}_\gamma \times \epsilon(\mathbf{k}_\gamma, \sigma_\gamma)]\mathcal{Z}_0, \quad (35)$$

where $\mathcal{Z}_0$ involves an integral over meson wave functions, the scalar function $K^1(k,q)$, the gluon absorption kernel and the Green's function $1/\Delta E$.

TABLE II. Expected decay widths for the nonzero hybrid-to-meson radiative transitions. The input charmonium meson masses have been taken from the nonrelativistic model in [26] and the mass of the hybrid multiplet was set to $m_{\rm hyb} = 4.35$ GeV.

Transition	Γ for κ_1 (keV)	Γ for κ_2 (keV)
$(Y \to \eta_c\gamma)_{M_1}$	39	126
$(0^{-+} \to J/\psi\gamma)_{M_1}$	32	116
$(\eta_{c_1} \to J/\psi\gamma)_{M_1}$	32	116
$(2^{-+} \to J/\psi\gamma)_{M_1}$	32	116

The quantity κ_1^2 defined by

$$\Gamma(Y \to \eta_c \gamma)_{M_1} = \alpha k_\gamma^3 \kappa_1^2 \tag{36}$$

can be compared with the lattice result given in Eq. (33),

$$\kappa_1 = \frac{1}{32\sqrt{3}\pi^{\frac{3}{2}} m_q} \frac{|\mathcal{Z}_0|}{m_Y} = \frac{8}{3\sqrt{3}} \frac{|\hat{V}|}{(m_Y + m_{\eta_c})}. \tag{37}$$

This gives a relation between $\mathcal{Z}_0$ and the magnetic dipole form factor $\hat{V}$; using the lattice value of $\hat{V} = 0.28$ we obtain $\kappa_1^2 = 3.47 \times 10^{-3}$ GeV^{-2} and it corresponds to a decay width of $\Gamma(Y \to \eta_c \gamma)_{M_1} = 40$ keV. The difference between the reported value by lattice and this model is due to the values of the masses for the hybrid and meson states used to calculate the photon momentum. The reason we take the lattice measurement to normalize $\mathcal{Z}_0$ is because of uncertainties in its computation within the model. It requires knowledge of the hybrid wave function, which in turn requires solving the three-body problem; cf. Eq. (5). We leave this for future investigations and here focus instead on symmetry relations implied by the existence of the light hybrid multiplet.

Using the value for $|\mathcal{Z}_0|^2$ or equivalently κ_1^2 estimated above, we can now make a prediction for the other three nonzero hybrid radiative transitions that in our model are determined by the same wave function overlap. These are $0^{-+} \to J/\psi(1^{--})\gamma$, $\eta_{c1}(1^{-+}) \to J/\psi(1^{--})\gamma$ and $2^{-+} \to J/\psi(1^{--})\gamma$. The results are summarized in Table II.

2. $0^{-+} \to J/\psi(1^{--})\gamma$

This is also a dipole magnetic transition. As it is shown below, the model predicts that any difference with respect to $Y(1^{--}) \to \eta_c(0^{-+})\gamma$ is only due to the available phase space as determined by the magnitude of the photon momentum, k_γ. The matrix element for this transition is given by

$$\mathcal{M}_{N \to N'\gamma} = -\frac{e_q}{m_q} \frac{i\sqrt{3}}{64\pi^{\frac{3}{2}}} \epsilon_{M'} \cdot [\mathbf{k}_\gamma \times \epsilon(\mathbf{k}_\gamma, \sigma_\gamma)] \mathcal{Z}_0. \tag{38}$$

The normalized results for transition with respect to lattice magnetic dipole form factors are summarized in Table II.

3. $\eta_{c1}(1^{-+}) \to J/\psi(1^{--})\gamma$

The multipole decomposition for this transition includes a magnetic dipole and an electric quadrupole transition but to lowest order in photon momentum the magnetic dipole transition dominates. The corresponding matrix element is given by

$$\mathcal{M}_{N \to N'\gamma} = \frac{e_q}{m_q} \frac{3\sqrt{2}}{128\pi^{\frac{3}{2}}} (\epsilon_M^* \times \epsilon_{M'}) \cdot [\epsilon(\mathbf{k}_\gamma, \sigma_\gamma) \times \mathbf{k}_\gamma] \mathcal{Z}_0, \tag{39}$$

and the decay width is given by $\Gamma(\eta_{c1} \to J/\psi\gamma)_{M_1} = \alpha k_\gamma \kappa_2^2$, where we have defined κ_2 as

$$\kappa_2 \equiv \frac{k_\gamma}{32\sqrt{3}\pi^{\frac{3}{2}} m_q} \frac{|\mathcal{Z}_0|}{m_{\eta_{c1}}} = \frac{4}{3\sqrt{3}} \frac{|\hat{F}|}{m_{\eta_{c1}}}. \tag{40}$$

Using the lattice value $\hat{F} = 0.69$ GeV we find

$$\kappa_2^2 = 1.49 \times 10^{-2}. \tag{41}$$

We can now estimate the difference in $|\mathcal{Z}_0|^2$ obtained using the two lattice results as normalizers. We find

$$|\mathcal{Z}_0|_{\hat{F}} \approx 2 \times |\mathcal{Z}_0|_{\hat{V}}, \tag{42}$$

where the subscript indicates which lattice matrix element is used in the determination. This result implies significant dependence of $\mathcal{Z}_0$ on the process and can be interpreted as a measure of the difference in the wave functions of the 1^{--} and 1^{-+} hybrids. This discrepancy is also seen in the ratio $\mathcal{R} = \Gamma(Y \to \eta_c\gamma)/\Gamma(\eta_{c_1} \to J/\psi\gamma)$ which is approximately 0.37 on the lattice while our model predicts $\mathcal{R} \approx 1$ for the whole hybrid super multiplet. In Table II, we show the predictions for the decay widths normalized using both κ_1 and κ_2.

4. $2^{-+} \to J/\psi(1^{--})\gamma$

The hybrid 2^{-+} is the last remaining member of the lightest hybrid multiplet considered here. Since no pseudotensor charmonium transition has been observed (not even one fitting any of the ordinary $c\bar{c}$ meson multiplets), the results of this model may be relevant to future experimental searches. The matrix element corresponding to this transition is given by

$$\mathcal{M}_{N \to N'\gamma} = \frac{e_q}{m_q} \frac{3i}{64\pi^{\frac{3}{2}}} \epsilon_M^{*ij} \epsilon_{M'}^j [\mathbf{k}_\gamma \times \epsilon(\mathbf{k}_\gamma, \sigma_\gamma)]^i \mathcal{Z}_0. \tag{43}$$

The predictions are summarized in Table II.

C-violating hybrid transitions.—Two charge conjugation–violating matrix elements have been reported in [29]. Both involve the exotic hybrid and they are $1^{-+} \to 0^{-+}\gamma$ and $1^{-+} \to 0^{++}\gamma$. In our model the matrix element for the $1^{-+} \to 0^{-+}\gamma$ transition vanishes identically. The reason is that in the matrix element for the photon coupling to the quark i.e. the two terms in the curly brackets in Eq. (19) only the spin-flip term contributes but does not bring any gluon momentum ($\mathbf{k}$) contribution. Therefore, all the gluon momentum dependence comes from the Coulomb interaction Eq. (6) and the hybrid wave function Eq. (A2). Thus, after performing the gluon

TABLE III. C-violating expected amplitudes.

Transition	$\lvert\hat{E}_1\rvert$ for κ_3 [GeV]
$Y \to h_c\gamma$	0.60
$0^{-+} \to \chi_{c_1}\gamma$	0.34
$\eta_{c_1} \to \chi_{c_0}\gamma$	0.34
$\eta_{c_1} \to \chi_{c_1}\gamma$	0.30
$\eta_{c_1} \to \chi_{c_2}\gamma$	0.38
$2^{-+} \to \chi_{c_1}\gamma$	0.38
$2^{-+} \to \chi_{c_2}\gamma$	0.66

angular integration Eq. (C1), the transition matrix element gives exactly zero to the term proportional to $\sim\varepsilon_{ijk}\hat{\mathbf{q}}_g^i\hat{\mathbf{q}}_g^k = 0$.

The matrix elements for the other, nonvanishing C-violating transitions are summarized below:

$$\mathcal{M}_{Y\to h_c\gamma} = \kappa_3 e_q \frac{3i}{16(4\pi)^{\frac{3}{2}}}(\epsilon_M^* \times \epsilon_{M'})\cdot\epsilon(\mathbf{k}_\gamma,\sigma_\gamma),$$

$$\mathcal{M}_{0^{-+}\to\chi_{c1}\gamma} = \kappa_3 e_q \frac{\sqrt{6}}{16(4\pi)^{\frac{3}{2}}}\epsilon(\mathbf{k}_\gamma,\sigma_\gamma)\cdot\epsilon_{M'},$$

$$\mathcal{M}_{\eta_{c1}\to\chi_{c0}\gamma} = -\kappa_3 e_q \frac{\sqrt{6}}{16(4\pi)^{\frac{3}{2}}}\epsilon_M^*\cdot\epsilon(\mathbf{k}_\gamma,\sigma_\gamma),$$

$$\mathcal{M}_{\eta_{c1}\to\chi_{c1}\gamma} = -\kappa_3 e_q \frac{3i}{32(4\pi)^{\frac{3}{2}}}(\epsilon_M^* \times \epsilon_{M'})\cdot\epsilon(\mathbf{k}_\gamma,\sigma_\gamma),$$

$$\mathcal{M}_{\eta_{c1}\to\chi_{c2}\gamma} = \kappa_3 e_q \frac{3\sqrt{2}}{32(4\pi)^{\frac{3}{2}}}\varepsilon_{ijk}\varepsilon_{ilm}\epsilon_M^{*j}\epsilon^l(\mathbf{k}_\gamma,\sigma_\gamma)\epsilon_{M'}^{km},$$

$$\mathcal{M}_{2^{-+}\to\chi_{c1}\gamma} = \kappa_3 e_q \frac{3\sqrt{2}}{32(4\pi)^{\frac{3}{2}}}\varepsilon_{ijk}\varepsilon_{lkm}\epsilon_M^{*il}\epsilon^j(\mathbf{k}_\gamma,\sigma_\gamma)\epsilon_{M'}^{*m},$$

$$\mathcal{M}_{2^{-+}\to\chi_{c2}\gamma} = -\kappa_3 e_q \frac{3i}{16(4\pi)^{\frac{3}{2}}}\varepsilon_{ijk}\epsilon_M^{*il}\epsilon^j(\mathbf{k}_\gamma,\sigma_\gamma)\varepsilon_{M'}^{lk}, \quad (44)$$

where κ_3 is defined as

$$\kappa_3 \equiv \frac{N_c\sqrt{C_F}}{m_q}|\mathcal{Z}_1| = \frac{16(4\pi)^{\frac{3}{2}}}{\sqrt{6}}|\hat{E}_1|_{CV}. \quad (45)$$

It is observed that, as before, all matrix elements depend on a single wave function overlap factor $\mathcal{Z}_1$, given in the Appendix. To determine the common factor κ_3 for all the nonzero hybrid C-violating transitions found in our model we use the transition amplitude ($|\hat{E}_1|_{CV} = 0.34$ GeV) from lattice simulations reported for $1^{-+} \to 0^{++}\gamma$. Therefore, using Eq. (31), $\kappa_3 = 98.93$ GeV. The numerical results shown in Table III constitute predictions of the model.

IV. SUMMARY AND OUTLOOK

We studied radiative decays of conventional charmonia and charmonium hybrids. Ordinary $c\bar{c}$ mesons with quantum numbers J^{PC}, $\eta_c(0^{-+})$, $J/\psi(1^{--})$, $\chi_{c0}(0^{++})$, $\chi_{c1}(1^{++})$, $h_c(1^{+-})$, $\chi_{c2}(2^{++})$ were used as benchmarks where we considered the minimal coupling of the photon to the nonrelativistic quarks. Simple harmonic oscillator wave functions with fixed size parameters were used to calculate the decay widths. We have compared our results with other models [25,26] and found a reasonable agreement. A few new predictions for transition amplitudes were presented including charge-violating transition amplitudes.

To describe hybrid decays we considered a model based on an effective QCD Hamiltonian that describes nonrelativistic quarks interacting with (relativistic) gluons and is constructed from the QCD in the Coulomb gauge by applying Foldy-Wouthuysen transformation. We have derived all relevant matrix elements, which can be computed given a model for a hybrid meson wave function. We considered decays of states from the hybrid multiplet 1^{--}, $(0,1,2)^{-+}$ with 1^{-+} being the exotic state. There are 24 possible radiative transitions between this multiplet and ground state charmonia. The decay widths obtained in this model were normalized with respect to the two reported lattice transition amplitudes for $\Gamma(Y(1^{--}) \to \eta_c\gamma)$ and $\Gamma(\eta_{c1}(1^{-+}) \to J/\psi\gamma)$. The other two $\Gamma(0^{-+} \to J/\psi\gamma)$ and $\Gamma(2^{-+} \to J/\psi\gamma)$ constitute predictions of the model. In general the model predicts $\mathcal{R} = \frac{\Gamma(N\to N'\gamma)}{\Gamma(\eta_{c1}(1^{-+})\to J/\psi\gamma)} \approx 1$ for the whole hybrid multiplet while lattice reports $\mathcal{R} = \frac{\Gamma(Y(1^{--})\to\eta_c\gamma)}{\Gamma(\eta_{c1}(1^{-+})\to J/\psi\gamma)} = 0.37$. We also investigated C-violating matrix elements involving hybrids. The model predicts several of such matrix elements to be nonzero and we used the lattice transition amplitude for $\eta_{c1}(1^-+) \to 0^{++}\gamma$ as normalizer to constrain our predictions.

In the absence of spin-dependent interactions, the model leads to a degenerate hybrid multiplet. While this prediction is not too far from lattice findings, the differences in transition matrix elements obtained from lattice simulations can be used to probe the wave functions predicted by the model. This requires solving the hybrid meson Schrödinger equation. A simplified variational attempt has been made in [15] and in the future we hope to obtain a more realistic description of hybrid mesons' wave functions.

ACKNOWLEDGMENTS

This work was supported in part by CONACyT under Postdoctoral supports Grants No. 166115 and No. 203672, the U.S. Department of Energy under Grant No. DE-FG0287ER40365, and Indiana University Collaborative Research Grant. P. G. and A. P. S. acknowledge support from U.S. Department of Energy Contract No. DE-AC05-06OR23177, under which Jefferson Science Associates, LLC, manages and operates Jefferson Laboratory.

APPENDIX A: MESON AND HYBRID SPIN-ORBITAL WAVE FUNCTIONS

The conventional $c\bar{c}$ meson spin-orbital wave functions are given by

$$\chi^{JMPC}_{m_1,m_2}(0^{-+}) = \frac{1}{2\sqrt{2\pi}}[i\sigma_2]_{m_1m_2},$$
$$\chi^{JMPC}_{m_1,m_2}(1^{--}) = \frac{1}{2\sqrt{2\pi}}[\sigma(i\sigma_2)]_{m_1m_2}\cdot\epsilon_M,$$
$$\chi^{JMPC}_{m_1,m_2}(0^{++}) = -\frac{1}{2\sqrt{2\pi}}[\sigma(i\sigma_2)]_{m_1m_2}\cdot\hat{\mathbf{q}},$$
$$\chi^{JMPC}_{m_1,m_2}(1^{++}) = -\frac{\sqrt{3}}{4\sqrt{\pi}}[\sigma\sigma_2]_{m_1m_2}\cdot\hat{\mathbf{q}}\times\epsilon_M,$$
$$\chi^{JMPC}_{m_1,m_2}(1^{+-}) = \frac{\sqrt{3}}{2\sqrt{2\pi}}[i\sigma_2]_{m_1m_2}\hat{\mathbf{q}}\cdot\epsilon_M,$$
$$\chi^{JMPC}_{m_1,m_2}(2^{++}) = \frac{\sqrt{3}}{2\sqrt{2\pi}}\sum_{ij}[\sigma^i(i\sigma_2)]_{m_1m_2}\hat{\mathbf{q}}^j\epsilon^{ij}_M. \tag{A1}$$

The hybrid spin-orbital wave functions are given by

$$\begin{aligned}
&\chi^{*JMPC}_{m_1,m_2,\sigma}(1^{--})\\
&\quad= -\frac{\sqrt{3}}{8\pi}[i\sigma_2]_{m_2m_1}\epsilon(-\mathbf{k},\sigma)\cdot\epsilon^*_M[\delta_{\sigma,1}-\delta_{\sigma,-1}],\\
&\chi^{*JMPC}_{m_1,m_2,\sigma}(0^{-+})\\
&\quad= \frac{1}{8\pi}[(i\sigma_2)\sigma]_{m_2m_1}\cdot\epsilon(-\mathbf{k},\sigma)[\delta_{\sigma,1}-\delta_{\sigma,-1}],\\
&\chi^{*JMPC}_{m_1,m_2,\sigma}(1^{-+})\\
&\quad= \frac{\sqrt{3}}{8\pi\sqrt{2}}[\sigma_2\sigma]_{m_2m_1}\cdot\epsilon(-\mathbf{k},\sigma)\times\epsilon^*_M[\delta_{\sigma,1}-\delta_{\sigma,-1}],\\
&\chi^{*JMPC}_{m_1,m_2\sigma}(2^{-+})\\
&\quad= -\frac{\sqrt{3}}{8\pi}\sum_{ij}[(i\sigma_2)\sigma^j]_{m_2m_1}\epsilon^i(-\mathbf{k},\sigma)\epsilon^{*ij}_M[\delta_{\sigma,1}-\delta_{\sigma,-1}].
\end{aligned} \tag{A2}$$

APPENDIX B: MESON-TO-MESON RELEVANT EXPRESSIONS

The radiative transitions between two conventional mesons produce the following set integrations:

$$\int\frac{d\mathbf{q}}{(2\pi)^3}\Psi^{N,\alpha}_{c\bar{c}}(q)\Psi^{N',\alpha'}_{c\bar{c}}(q) = \mathcal{J},$$
$$\int\frac{d\mathbf{q}}{(2\pi)^3}\Psi^{N,\alpha}_{c\bar{c}}(q)\Psi^{N',\alpha'}_{c\bar{c}}\left(\left|\mathbf{q}-\frac{\mathbf{k}_\gamma}{2}\right|\right)\hat{\mathbf{q}}^i\hat{\mathbf{q}}^j = \mathcal{A}\delta_{ij}+\mathcal{B}\hat{\mathbf{k}}^i_\gamma\hat{\mathbf{k}}^j_\gamma,$$
$$\int\frac{d\mathbf{q}}{(2\pi)^3}\Psi^{N,\alpha}_{c\bar{c}}(q)\Psi^{N',\alpha'}_{c\bar{c}}\left(\left|\mathbf{q}-\frac{\mathbf{k}_\gamma}{2}\right|\right)q\hat{\mathbf{q}}^i\hat{\mathbf{q}}^j = \mathcal{D}\delta_{ij}+\mathcal{G}\hat{\mathbf{k}}^i_\gamma\hat{\mathbf{k}}^j_\gamma, \tag{B1}$$

and

$$\begin{aligned}
\mathcal{A} &= \int\frac{d\mathbf{q}}{(2\pi)^3}\Psi^{N,\alpha}_{c\bar{c}}(q)\Psi^{N',\alpha'}_{c\bar{c}}\left(\left|\mathbf{q}-\frac{\mathbf{k}_\gamma}{2}\right|\right)\left(\frac{1-\hat{y}^2}{2}\right)\\
\mathcal{B} &= \int\frac{d\mathbf{q}}{(2\pi)^3}\Psi^{N,\alpha}_{c\bar{c}}(q)\Psi^{N',\alpha'}_{c\bar{c}}\left(\left|\mathbf{q}-\frac{\mathbf{k}_\gamma}{2}\right|\right)\left(\frac{3\hat{y}^2-1}{2}\right),\\
\mathcal{D} &= \int\frac{d\mathbf{q}}{(2\pi)^3}\Psi^{N,\alpha}_{c\bar{c}}(q)\Psi^{N',\alpha'}_{c\bar{c}}\left(\left|\mathbf{q}-\frac{\mathbf{k}_\gamma}{2}\right|\right)q\left(\frac{1-\hat{y}^2}{2}\right),\\
\mathcal{G} &= \int\frac{d\mathbf{q}}{(2\pi)^3}\Psi^{N,\alpha}_{c\bar{c}}(q)\Psi^{N',\alpha'}_{c\bar{c}}\left(\left|\mathbf{q}-\frac{\mathbf{k}_\gamma}{2}\right|\right)q\left(\frac{3\hat{y}^2-1}{2}\right),
\end{aligned} \tag{B2}$$

where $\hat{y} = \hat{\mathbf{q}}\cdot\hat{\mathbf{k}}_\gamma$.

APPENDIX C: HYBRID-TO-MESON RELEVANT EXPRESSIONS

In the hybrid-to-meson radiative transition, the integrals over the direction of gluon momentum produce the following set of relations:

$$\begin{aligned}
&\int d\hat{\mathbf{k}}K^{(1)}\left(\left|\frac{\mathbf{k}}{2}+\mathbf{q}_g\right|,\left|\frac{\mathbf{k}}{2}-\mathbf{q}_g\right|\right)\hat{\mathbf{k}}^i\hat{\mathbf{k}}^j\\
&\quad= \mathcal{A}(k,q_g)\delta_{ij}+\mathcal{B}(k,q_g)\hat{\mathbf{q}}^i_g\hat{\mathbf{q}}^j_g,
\end{aligned} \tag{C1}$$

with $\mathbf{q}_g = (\mathbf{q}'-\mathbf{q}+\frac{\mathbf{k}_\gamma}{2})$ and $x = \hat{\mathbf{q}}_g\cdot\hat{\mathbf{k}}$

$$\mathcal{A}(k,q_g) = \int d\hat{\mathbf{k}}K^{(1)}\left(\left|\frac{\mathbf{k}}{2}+\mathbf{q}_g\right|,\left|\frac{\mathbf{k}}{2}-\mathbf{q}_g\right|\right)\frac{1-x^2}{2},$$
$$\mathcal{B}(k,q_g) = \int d\hat{\mathbf{k}}K^{(1)}\left(\left|\frac{\mathbf{k}}{2}+\mathbf{q}_g\right|,\left|\frac{\mathbf{k}}{2}-\mathbf{q}_g\right|\right)\frac{3x^2-1}{2}. \tag{C2}$$

To leading order in photon momentum ($q_g\to|\mathbf{q}'-\mathbf{q}|$) we use the following notation:

$$\begin{aligned}
\mathcal{Z}_0 &= g^2\int\frac{k^2dk}{(2\pi)^3}\frac{d\mathbf{q}}{(2\pi)^3}\frac{d\mathbf{q}'}{(2\pi)^3}\Psi^{N,\alpha}_{c\bar{c}g}(k,q)\Psi^{N',\alpha'}_{c\bar{c}}(q')\\
&\quad\times\frac{k}{\sqrt{\omega_k}(\Delta E)}\mathcal{A}(k,|\mathbf{q}'-\mathbf{q}|).
\end{aligned} \tag{C3}$$

The dependence on the QCD coupling g^2 is a consequence of the presence of the gluon in the hybrid meson wave function as discussed in Sec. II.

1. Hybrid-to-meson *C*-violating relations

The *C*-violating transitions are given by terms proportional to $\mathcal{A}(k,|\mathbf{q}'-\mathbf{q}|)(q'-q)^i\hat{\mathbf{q}}'^j$; thus, the expressions in the *C*-violating hybrid-to-meson transitions can be simplified to

$$\mathcal{Z}_1 = \frac{g^2}{3}\int \frac{k^2 dk}{(2\pi)^3}\frac{d\mathbf{q}}{(2\pi)^3}\frac{d\mathbf{q}'}{(2\pi)^3}\Psi^{N,\alpha}_{c\bar{c}g}(k,q)\Psi^{N',\alpha'}_{c\bar{c}}(q') \times \frac{k}{\sqrt{\omega_k}(\Delta E)}\mathcal{A}(k,|\mathbf{q}'-\mathbf{q}|)(q'-q\hat{z}). \quad \text{(C4)}$$

APPENDIX D: MULTIPOLE DECOMPOSITION AND WIDTH DECAY

We need to determine the type of transition through the multipole decomposition. The simplest way is to consider that the photon moves in the $-\hat{\mathbf{z}}$ direction as in [27], so that the multipole decomposition is given by

$$\mathcal{M}(\lambda_\gamma = \pm) = \sum_l \sqrt{\frac{2l+1}{2J+1}}\langle l \mp 1, J'\lambda \pm 1 | J\lambda\rangle \times \left[E_l \frac{1}{2}(1+(-1)^l\delta P) \mp M_l \frac{1}{2}(1-(-1)^l\delta P)\right], \quad \text{(D1)}$$

where the transition can be represented as $(J\lambda) \to (J'\lambda') + (\gamma\lambda_\gamma)$, and δP is the product of the initial and final meson parities.

[1] D. Horn and J. Mandula, Phys. Rev. D **17**, 898 (1978).
[2] N. Isgur and J. E. Paton, Phys. Rev. D **31**, 2910 (1985).
[3] Y. A. Simonov, Nucl. Phys. **B592**, 350 (2000).
[4] A. Szczepaniak, E. S. Swanson, C. R. Ji, and S. R. Cotanch, Phys. Rev. Lett. **76**, 2011 (1996).
[5] F. Buisseret and C. Semay, Phys. Rev. D **74**, 114018 (2006).
[6] F. Brau and C. Semay, Phys. Rev. D **70**, 014017 (2004).
[7] C. J. Morningstar and M. J. Peardon, Phys. Rev. D **60**, 034509 (1999).
[8] M. Foster and C. Michael, Phys. Rev. D **59**, 094509 (1999).
[9] G. S. Bali and A. Pineda, Phys. Rev. D **69**, 094001 (2004).
[10] E. Eichten and F. Feinberg, Phys. Rev. D **23**, 2724 (1981).
[11] T. D. Lee, *Particle Physics and Introduction to Field Theory* (Harwood Academic, New York, 1981).
[12] F. J. Llanes-Estrada and S. R. Cotanch, Phys. Lett. B **504**, 15 (2001).
[13] I. J. General, S. R. Cotanch, and F. J. Llanes-Estrada, Eur. Phys. J. C **51**, 347 (2007).
[14] P. Guo, A. P. Szczepaniak, G. Galata, A. Vassallo, and E. Santopinto, Phys. Rev. D **77**, 056005 (2008).
[15] P. Guo, A. P. Szczepaniak, G. Galata, A. Vassallo, and E. Santopinto, Phys. Rev. D **78**, 056003 (2008).
[16] C. Feuchter and H. Reinhardt, Phys. Rev. D **70**, 105021 (2004).
[17] H. Reinhardt and C. Feuchter, Phys. Rev. D **71**, 105002 (2005).
[18] D. Zwanziger, Phys. Rev. Lett. **90**, 102001 (2003).
[19] J. Greensite and S. Olejnik, Phys. Rev. D **67**, 094503 (2003).
[20] V. Crede and C. A. Meyer, Prog. Part. Nucl. Phys. **63**, 74 (2009).
[21] V. Mathieu, N. Kochelev, and V. Vento, Int. J. Mod. Phys. E **18**, 1 (2009).
[22] E. S. Swanson, Phys. Rep. **429**, 243 (2006).
[23] E. Eichten, K. Gottfried, T. Kinoshita, K. D. Lane, and T. M. Yan, Phys. Rev. D **17**, 3090 (1978).
[24] E. Eichten, K. Gottfried, T. Kinoshita, K. D. Lane, and T. M. Yan, Phys. Rev. D **21**, 203 (1980).
[25] E. J. Eichten, K. Lane, and C. Quigg, Phys. Rev. Lett. **89**, 162002 (2002).
[26] T. Barnes, S. Godfrey, and E. S. Swanson, Phys. Rev. D **72**, 054026 (2005).
[27] J. J. Dudek, R. G. Edwards, and D. G. Richards, Phys. Rev. D **73**, 074507 (2006).
[28] J. J. Dudek, R. G. Edwards, N. Mathur, and D. G. Richards, Phys. Rev. D **77**, 034501 (2008).
[29] J. J. Dudek, R. G. Edwards, and C. E. Thomas, Phys. Rev. D **79**, 094504 (2009).
[30] J. J. Dudek, Phys. Rev. D **84**, 074023 (2011).
[31] F. L. Feinberg, Phys. Rev. D **17**, 2659 (1978).
[32] A. P. Szczepaniak and E. S. Swanson, Phys. Rev. D **65**, 025012 (2001).
[33] A. P. Szczepaniak, Phys. Rev. D **69**, 074031 (2004).
[34] C. Feuchter and H. Reinhardt, Phys. Rev. D **70**, 105021 (2004).
[35] H. Reinhardt and C. Feuchter, Phys. Rev. D **71**, 105002 (2005).
[36] W. Schleifenbaum, M. Leder, and H. Reinhardt, Phys. Rev. D **73**, 125019 (2006).
[37] D. Epple, H. Reinhardt, and W. Schleifenbaum, Phys. Rev. D **75**, 045011 (2007).
[38] D. Epple, H. Reinhardt, W. Schleifenbaum, and A. P. Szczepaniak, Phys. Rev. D **77**, 085007 (2008).
[39] A. P. Szczepaniak and P. Krupinski, Phys. Rev. D **73**, 116002 (2006).
[40] A. P. Szczepaniak and P. Krupinski, Phys. Rev. D **73**, 034022 (2006).
[41] K. J. Juge, J. Kuti, and C. J. Morningstar, Nucl. Phys. B, Proc. Suppl. **63**, 326 (1998).
[42] N. Brambilla *et al.*, Eur. Phys. J. C **71**, 1534 (2011).
[43] N. Brambilla *et al.*, arXiv:1404.3723.
[44] J. Beringer *et al.* (Particle Data Group), Phys. Rev. D **86**, 010001 (2012).
[45] Y. F. Gu and S. F. Tuan, arXiv:hep-ph/9910423.
[46] N. Brambilla *et al.*, arXiv:hep-ph/0412158v2.
[47] T. A. Armstrong *et al.* (E760 Collaboration), Nucl. Phys. **B373**, 35 (1992); Phys. Rev. Lett. **68**, 1468 (1992).

[48] J. Z. Bai *et al.* (BES Collaboration), Phys. Rev. Lett. **81**, 3091 (1998); Phys. Rev. D **60**, 072001 (1999).
[49] N. E. Adam *et al.*, Phys. Rev. Lett. **94**, 232002 (2005).
[50] J. L. Rosner *et al.* (CLEO Collaboration), Phys. Rev. Lett. **95**, 102003 (2005).
[51] S. Dobbs *et al.* (CLEO Collaboration), Phys. Rev. Lett. **101**, 182003 (2008).
[52] M. Ablikim *et al.* (BESIII Collaboration), Phys. Rev. Lett. **104**, 132002 (2010).
[53] B. Aubert *et al.* (*BABAR* Collaboration), Phys. Rev. D **74**, 091103 (2006).